ARMY RESEARCH LABORATORY

Deformation of a Coarse-Aggregate Barrier Subjected to Ballistic Impact Loading

by Todd W. Bjerke

ARL-TR-1346

April 1997

19970527 071

Army Research Laboratory
Aberdeen Proving Ground, MD 21005-5066

Deformation of a Coarse-Aggregate Barrier Subjected to Ballistic Impact Loading

Todd W. Bjerke
Weapons and Materials Research Directorate, ARL

Abstract

An experiment-oriented investigation aimed at gaining insight and understanding of the physical phenomena that occur when a projectile impacts a thin barrier consisting of a uniform, coarse aggregate was performed at the U.S. Army Research Laboratory. The thin barrier target was an assembly of solid steel cylinders oriented in a 15-by-15 rod square-packed array. Each cylinder had a length-to-diameter ratio of 3.5 and a serial number imprinted on its rear surface to permit barrier reconstruction after each shot. The projectile consisted of a solid aluminum cylinder with a diameter of approximately 2.5 aggregate diameters and a length of 1.25 aggregate element lengths. The impact velocity was 2 km/s. The data collected consisted of the crater size in the barrier (obtained from post-test reconstruction), plastic deformation of individual cylinders, and the residual penetrator length. A detailed analysis of the damage inflicted on the aggregate elements of the barrier was performed. Iso-strain contours were mapped on the face of the barrier to shed insight into the contact mechanics of the aggregate elements. A semi-empirical aggregate deformation model was created. The expected influence of impact velocity on aggregate deformation has been proposed and added to the semi-empirical model.

TABLE OF CONTENTS

INTENTIONALLY LEFT BLANK.

LIST OF FIGURES

INTENTIONALLY LEFT BLANK.

1. INTRODUCTION

The physical understanding of the damage inflicted to a protective barrier resulting from impact with a projectile is paramount to the intelligent design of advanced protective systems. The configuration of the protective barrier used for ballistic impact studies depends upon the overall protective device that the barrier is to represent. Although many barriers are homogeneous in configuration, a much broader class of barriers involves a nonuniform agglomeration of components. Such barriers can conceivably represent the means of protection for ammunition bunkers, nuclear reactors, armored military vehicles, or any asset for which protection against projectile impact is desired. Understanding the physical mechanisms present during the ballistic impact event requires an examination of the barrier penetration process as well as the lateral propagation of damage away from the impact crater. By having a clear understanding of the nature and behavior of the damage mechanisms present during such a ballistic impact event, the designer of a protective barrier system is then able to exploit these mechanisms to create a superior design.

The situation of an aggregate barrier with relatively large elements being impacted by a projectile at a velocity sufficient to produce erosion and gross plastic deformation was performed by the U.S. Army Research Laboratory (ARL). The experiment-oriented investigation used a simplistic protective barrier configuration, which was limited to an assembly of solid steel cylinders oriented in a 15-by-15 rod square-packed array. The projectile was a solid aluminum right-circular cylinder, which impacted the barrier cylinders end-on. The granularity of the barrier aggregate was such that approximately 2.5 of the steel cylinders would fit across the diameter of the projectile. An impact velocity of 2 km/s was chosen to ensure that significant erosion and plastic deformation of the barrier and projectile would occur.

2. BALLISTIC EXPERIMENT

The ballistic experiment consisted of impacting a solid aluminum projectile into an array of solid steel cylinders at a nominal velocity of 2 km/s. The experiment was performed in the ARL

1

high-pressure gun facility at Range 309A. Details of the facility are given by Bauer and Nagy [1]. The gun consists of a nominal 50-mm-diameter by 6-m-travel smoothbore powder gun with a large-capacity, high-pressure powder chamber. The gun empties into an impact chamber at atmospheric pressure. The target that represented the protective barrier was located approximately 4.5 m from the gun muzzle. A stack of plywood with a thickness of 600 mm was placed 2 m downrange of the target to serve as a soft recovery medium for the penetrator and target debris.

One piezoelectric and two copper crusher pressure gauges were located in the powder chamber of the gun to aid with the internal ballistic diagnostics of the gun. Two 150-kV orthogonal flash x-ray shadowgraph systems, located approximately 450 and 760 mm uprange of the target, were used to provide penetrator attitude and velocity data prior to impact. A 1-MV single-plane x-ray shadowgraph system was placed at the same downrange location as the target and was used to provide a side-view image of the target during the impact event. The x-ray systems required a means for detecting and enunciating the arrival of the penetrator at the x-ray stations (i.e., a properly timed trigger to activate each system). The trigger system employed was a "break-screen" placed approximately 300 mm uprange of the first x-ray station. The break-screen consisted of a piece of paper with a conductive etching on it, mounted on a thin piece of cardboard located on the shotline of the gun. A voltage is applied across the etching and is monitored for interruptions. When the penetrator strikes the break-screen, it perforates the cardboard and interrupts the electrical circuit across the screen. This interruption activates the delay generators used to pulse the flash x-ray systems.

The penetrator consisted of a solid right-circular cylinder of 6061-T6 aluminum alloy with a length of 76.2 mm, a diameter of 46.9 mm, and a mass of 356.1 g. The aluminum penetrator was placed in a plastic cup made of Polypropylux 944. The cup had a wall thickness of 1.6 mm, a base thickness of 6.4 mm, and a mass of 30.1 g. The cup served as a sabot and obturator and was not discarded during the flight of the penetrator.

The target which represented the protective barrier consisted of 225 solid steel cylinders contained within a polyethylene frame. Each of the steel cylinders was made from 4130 annealed steel and had a diameter of 17.45 mm and a length of 61.0 mm. The cylinders were placed in the plastic frame with a square-packed configuration, with the principal axes of the square-packing in the horizontal and vertical directions. These directions are referred to herein as the x and y directions, respectively. A photograph of the target is shown in Figure 1. The packing configuration yielded a target with 15 rods each in the vertical and horizontal direction. A unique serial number was imprinted on the rear face (downrange facing end) of each steel cylinder. Care was taken during assembly of the target to ensure that proper orientation of the serial numbers was maintained. This permitted an accurate reconstruction of the target after the impact event. The plastic frame used to contain the steel cylinders had a wall thickness of 11.4 mm and a length equivalent to that of the steel cylinders (61 mm). Steel screws were used to fasten the ends of the plastic pieces together. The target was placed in the impact chamber such that the aim point of the gun was the center of the target front face. The target was at normal incidence (no obliquity). The target was instrumented with a pair of strain gauges attached to two different steel cylinders located along the vertical axis of symmetry of the target using a cyanoacrylate-based adhesive. The two gauges were used as time-of-arrival indicators for determining the propagation velocity of a stress wave traversing laterally through the target. The gauges were used solely for timing information and were not properly configured to yield meaningful strain measurements.

The ballistic test procedure used was typical of conventional ballistic range impact testing in that the penetrator was accelerated to the desired velocity in the gun and permitted to pass through the instrumentation field, perforate the target, and then embed itself in the thick plywood stack placed downrange of the target. A projectile velocity of 2.01 km/s and a yaw of less than 0.5° were determined from the x-ray shadowgraphs and associated timing information. The projectile velocity was assumed not to decrease significantly during the short flight distance between the x-ray stations and the target; hence, the velocity obtained from the x-ray systems was used as the impact velocity. The strain gauge response timing data yielded a wave propagation velocity of 1.14 km/s.
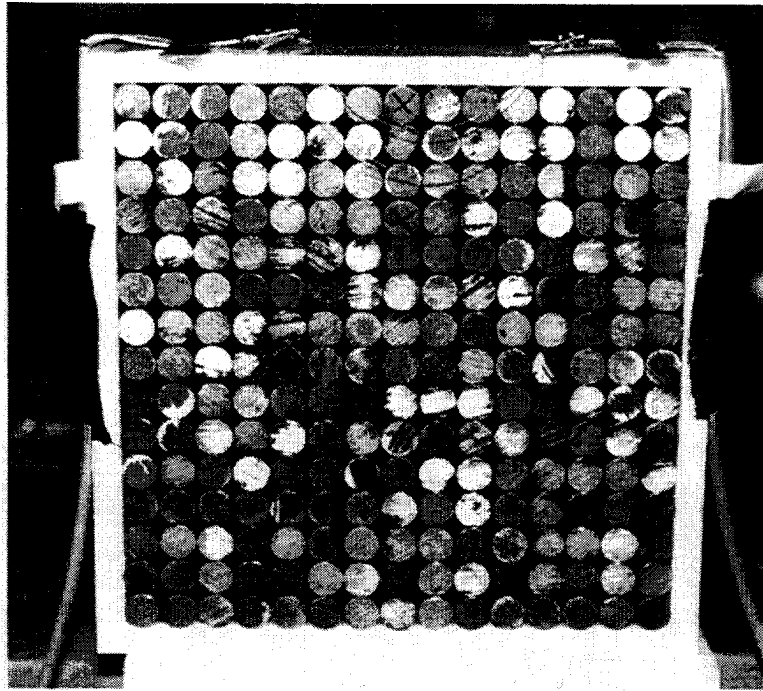
Figure 1. Target configuration.

The side-view x-ray image of the target taken during the impact event is shown in Figure 2. The image was taken approximately 90 µs after impact. The projectile was traveling from left to right in the image. The right (downrange) side of the target image shows steel cylinders in the center of the target translated in the downrange direction. These cylinders are also rotated in such a way that their uprange ends have been moved laterally towards the edge of the barrier array (i.e., rotated away from the crater region).

The target was reconstructed after the impact event by collecting all of the individual steel cylinders and placing them in a large piece of foam which had shallow holes arranged in a 15-by-15 array. The downrange end of each cylinder (the end that was imprinted with a serial number) was placed in the hole corresponding to its pre-impact location in the array, which permitted the impacted end of each cylinder to be visible. The reconstructed target is shown in Figure 3. All of the steel cylinders were recovered. The penetrator did not erode the full length of the cylinders located in the impact crater region of the target. The center cylinder of the target
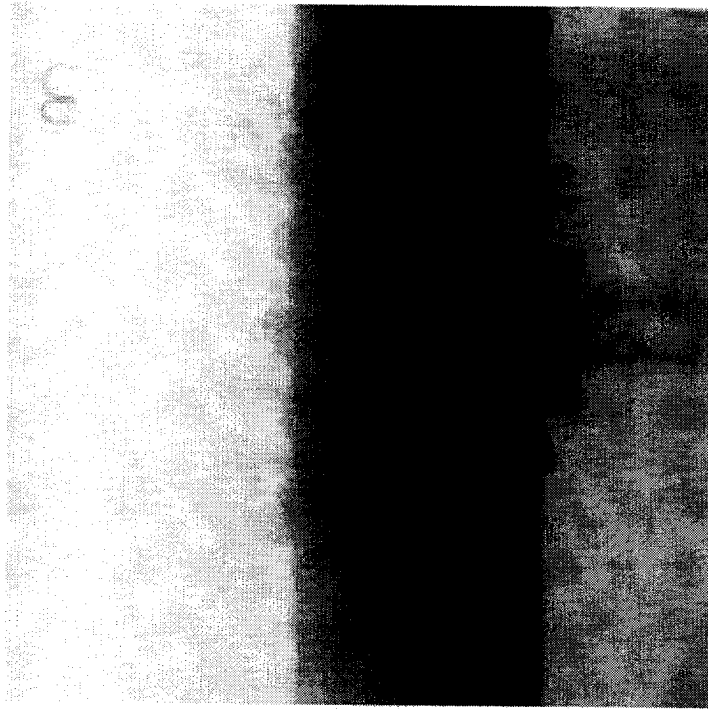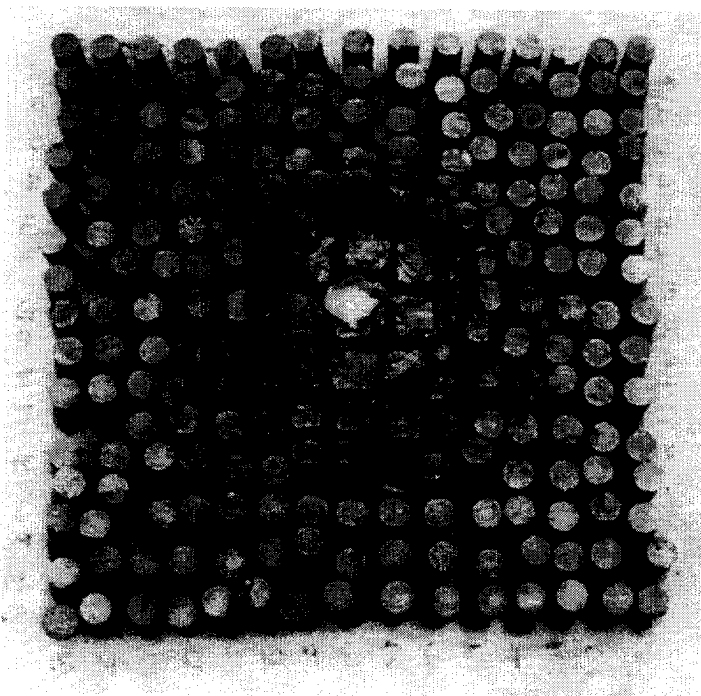
4

Figure 2. Side-view x-ray image of target.

Figure 3. Reconstructed target.

5

had a length of 34 mm (56% of the original length). The impact crater had a diameter spanning the width of five steel cylinders (87 mm). The aluminum penetrator was not completely consumed during the impact event and was recovered from the stack of plywood. The measured residual length of the penetrator was 18.8 mm (25% of the original length).

3. BARRIER DAMAGE ANALYSIS

A detailed analysis of the damage inflicted on each of the aggregate elements was performed. The length of each steel cylinder was measured and is shown in Figure 4. The measured lengths of the cylinders adjacent to the crater edge were greater than their original lengths. The longest cylinder was stretched 138% of its original length. These elongated cylinders had one side with an irregular, eroded surface coated with aluminum deposits. This side corresponded to the side that formed the impact crater wall. The opposite side had a deformed shape, which indicated that the cylinder was pressed against its nearest neighbor in the radial direction with significant pressure. These observations led to the conclusion that the impact forces that cause target cratering also accelerate cylinders in the downrange direction while applying lateral pressure, resulting in cylinder elongation.
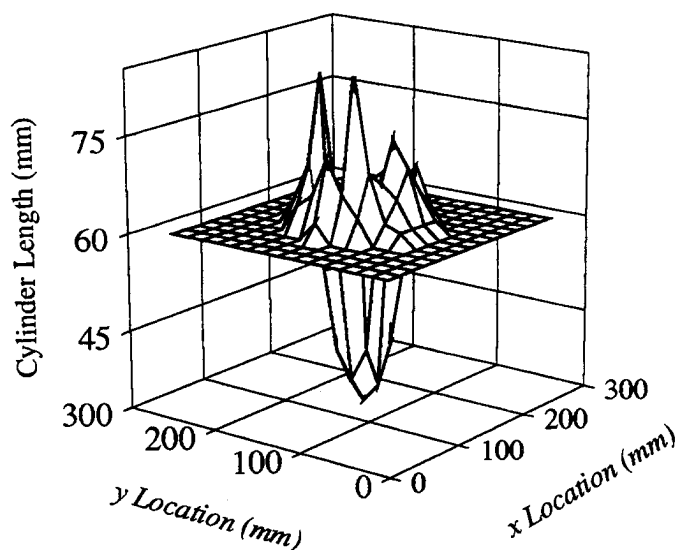

Figure 4. Measured steel cylinder length.

6

The extent of lateral deformation to each of the barrier aggregate elements was determined next. The diameter of each steel cylinder located outside the impact crater was measured in the x and y directions. These diameter measurements were made at three locations along the length of the cylinder: the front, middle, and rear, as shown in Figure 5. The level of plastic strain at each measurement location on the cylinder was determined using equation (1):

$$\epsilon = \left| \ln\left(\frac{d_x}{d_o}\right) \right| + \left| \ln\left(\frac{d_y}{d_o}\right) \right|,$$ (1)

where ϵ is the total strain at the measurement location, d_x and d_y are the cylinder diameter measurements in the x and y directions, and d_o is the original cylinder diameter. The absolute values of the x and y components of the strain were taken to permit a summation of the compressive and tensile strains. This yields a value of strain indicative of the total level of cylinder plastic deformation for the particular measurement location. Natural strains (those obtained using the natural logarithm function) were calculated because many of the cylinders experienced large strains. The values of ϵ determined for each of the three measurement locations were then numerically averaged together to obtain an average value of strain, ϵ_{avg}, for each cylinder in the target.
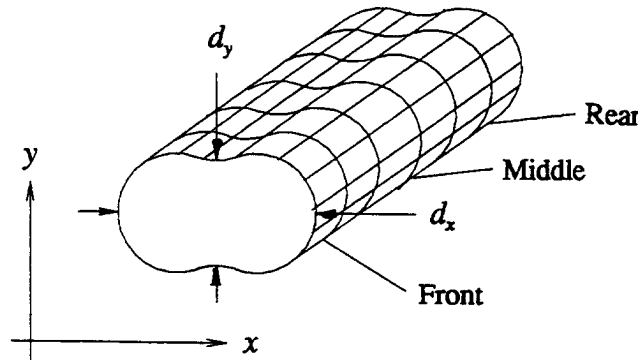

Figure 5. Steel cylinder diameter measurements.

7

The value of ϵ_{avg} for each of the cylinders in the target (located outside the impact crater) was used to create an iso-strain contour map, shown in Figure 6. The contour map shows lines of constant strain for ϵ_{avg} ranging from 0.1 to 0.001. There are several unique features of the iso-strain contours. The lines of constant strain tend to be linear and oriented at a 45° angle to the packing axes of the target. The contours form a series of concentric diamond-shaped polygons with the peaks of the polygons aligned with the two axes of symmetry of the target. The cylinder-to-cylinder contact paths along the two axes of symmetry of the target are linear. The iso-strain contours suggest that stress waves propagating radially outward from the impact crater are dissipated least along these paths. Furthermore, the value of ϵ_{avg} determined for each cylinder appears to be dependent upon the number of cylinder-to-cylinder contacts that the stress wave must propagate across. For example, looking at Figure 6, the number of cylinder-to-cylinder contacts to get to the top peak of the 0.1 strain contour is six (starting at the center of the target). An ϵ_{avg} value of 0.1 exists for any cylinder in the target that is six cylinder-to-cylinder contacts from the target center, whether the path chosen is horizontal, vertical, or a combination of both. Traversing three vertical contacts and three horizontal contacts yields a cylinder with a strain of 0.1, as does traversing four vertical and two horizontal contacts, or five vertical and one horizontal contact, or six horizontal contacts. Thus, if the variation of ϵ_{avg} is known for the cylinders located along the axes of symmetry of the target, then ϵ_{avg} for all other cylinders can be determined.

The two axes of symmetry of the target yield four linear cylinder contact-to-contact paths emanating from the center of the target. The value of ϵ_{avg} for the cylinders along these four paths is shown as a function of distance from the target center in Figure 7. The distance from the target center is shown in terms of the number of cylinders from the target center, with the center cylinder denoted as cylinder number zero. The first cylinder outside of the impact crater was cylinder number three. An equation was fit to the data that had the following form:

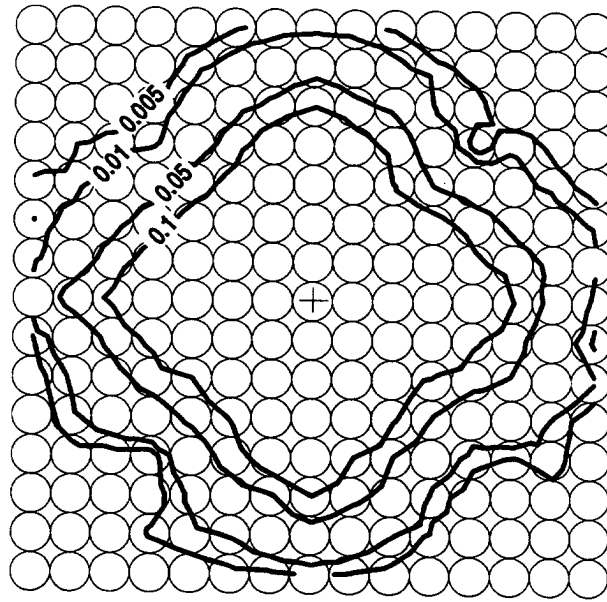$$\epsilon_{avg} = a + \frac{b}{r^2}, \qquad (2)$$
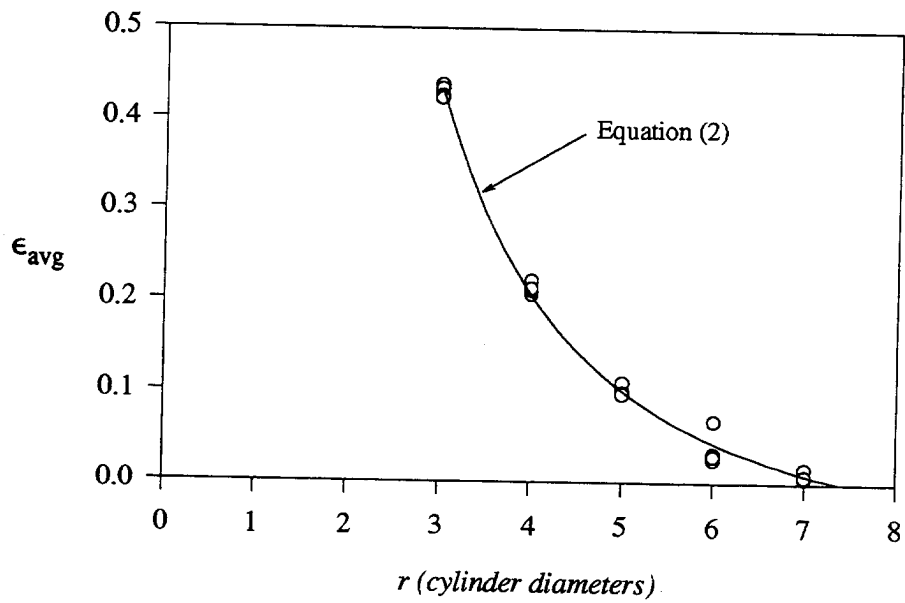
Figure 6. Target iso-strain contour plot.

Figure 7. ϵ_{avg} decay along target axes of symmetry.

9

where ϵ_{avg} is the average strain assigned to each cylinder, r is the radial distance from the target center in terms of number of cylinders, and a and b are empirical fitting parameters. Equation (2) is shown in Figure 7. The values of a and b that gave the results shown are -0.086 and 4.67, respectively. The form of equation (2) and the goodness of fit to the data suggest that ϵ_{avg} decays along the target axes of symmetry at a rate proportional to the square of the inverse of the distance from the crater center. This is characteristic of a radially expanding two-dimensional stress wave, decreasing in intensity as it expands.

4. INFLUENCE OF IMPACT VELOCITY

A combination of equation (2) and the unique features of the iso-strain contour map shown in Figure 6 enable the value of ϵ_{avg} to be determined for any of the cylinders in the target that are located outside the impact crater. This combination also provides a rudimentary insight into the mechanics present during the impact event that lead to barrier aggregate deformation. However, this is for only one impact velocity and a single projectile-target configuration, and thus serves merely as a starting point for a comprehensive understanding of such interactions. Of the many possible variations and extensions of the impact event that can be explored, one fundamental variation is impact velocity.

Several assumptions were made to develop a semi-empirical aggregate deformation model that embodies the influence of impact velocity. It was assumed that the fundamental phenomenon that produced cylinder deformation does not change with impact velocity. As the impact velocity is increased above 2 km/s, the target is expected to crater, radial stress waves are expected to propagate toward the lateral periphery of the target and decrease in intensity as they do so, and iso-strain contours of the same general shape as those observed in Figure 6 are expected due to the unique cylinder packing configuration. The general form of equation (2) is not expected to change (i.e., ϵ_{avg} along the target axes of symmetry is expected to be proportional to the square of the inverse of the distance from the crater center). Furthermore, the maximum value of ϵ_{avg} for the cylinders adjacent to the impact crater edge is not expected to increase with increasing impact velocity. The reason for this expectation is that the cylinders from the experiment that

were adjacent to the crater edge were deformed to the point where signs of material failure were becoming evident (i.e., cracks along the length and minor erosion of the top surface). From this observation, it can be concluded that cylinders adjacent to the crater edge can have a maximum ϵ_{avg} value of approximately 0.43 (the maximum value shown in Figure 7). If cylinders are strained beyond this approximate value, they experience material failure and become part of the crater region.

There are two features that are expected to be directly influenced by impact velocity: the final size of the impact crater and the empirical fitting parameters in equation (2). As the impact velocity is increased, the impact crater increases in diameter. This, in turn, shifts the curve shown in Figure 7 to the right. This shifted curve is also expected to modify in shape. Thus, the task at hand essentially consists of determining the rate of crater growth with impact velocity and the degree of change equation (2) should exhibit as impact velocity is varied. More specifically, how does Figure 7 change as the impact velocity is varied? Once this is determined, the iso-strain contours for the target can then be constructed and compared.

The relationship between impact crater diameter and impact velocity is given by Hohler and Stilp [2] as the following:

$$d_c \propto V^\alpha,$$
(3)

where d_c is the crater diameter, V is the impact velocity, and the exponent α is equivalent to 1 for a long penetrator impacting a finite target. Hence, crater diameter is linear with impact velocity. The translation of the curve shown in Figure 7 should then also be linear with impact velocity. Insight into the change in shape of equation (2) with impact velocity is deduced from Tate [3]. The impact cratering process was modeled by Tate using potential flow field theory. One of the conclusions from this approach was that the strain field surrounding a penetration cavity "scales linearly with the hole diameter." Thus, if the iso-strain contours of two targets are compared, one target with a crater diameter twice that of the other, the distance between lines of constant strain for the target with the larger crater should be twice that of the target with the smaller crater.

11

Equation (3) provides the link between crater diameter and velocity, thereby establishing that a linear relationship exists between the strain field and the impact velocity. Two manipulations of the curve shown in Figure 7 are required to account for changing impact velocity. The first is a translation of the curve to account for the linear growth of the crater with velocity. The second manipulation is a linear scaling, or stretching, of the x axis with impact velocity. These two manipulations were performed to create a series of curves for impact velocities ranging from 3 to 6 km/s, using the 2-km/s experiment as the baseline datum for the empirical correlations. These curves, along with the 2-km/s baseline curve, are shown in Figure 8. The value of ϵ_{avg} for the cylinders adjacent to the crater edge was maintained at 0.43, the maximum value from the 2-km/s experiment. Whether this value does in fact represent the maximum possible for all velocities should be verified in the future with additional experiments.
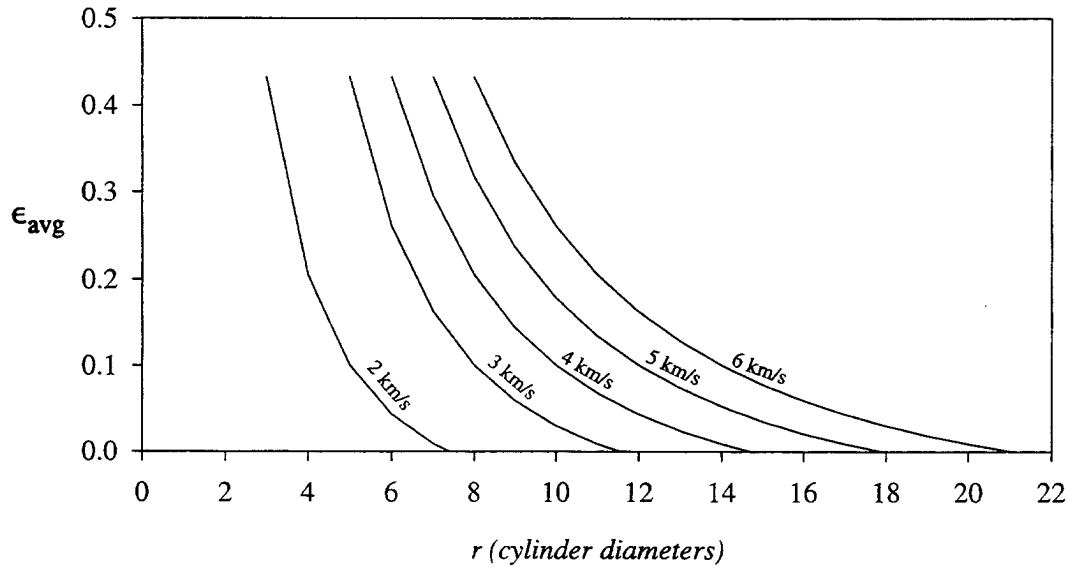
Figure 8. Velocity influence on ϵ_{avg} radial decay.

The curves shown in Figure 8, along with the assumptions discussed earlier, permit the construction of iso-strain contours for impact velocities ranging from 2 to 6 km/s. An example showing the change in plastic deformation of the barrier aggregate elements as impact velocity is increased from 2 km/s to 6 km/s is shown in Figure 9. A comparison of the iso-strain contours
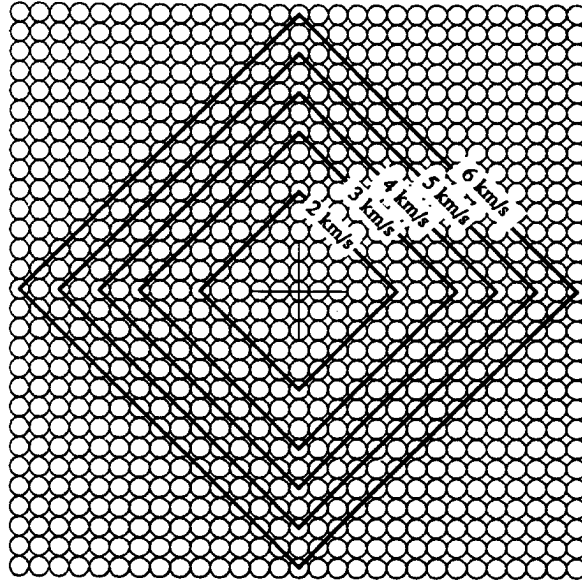
Figure 9. Velocity influence on $\epsilon_{avg} = 0.1$ contour.

corresponding to a ϵ_{avg} value of 0.1 for each of the impact velocities is made. This comparison illustrates the advancement of a particular ϵ_{avg} level as the impact velocity increases.

The utility of the process used to construct Figure 9 is the following. If a particular protective barrier consists of an assembly of aggregate elements, and if the elements are able to survive a specified level of plastic deformation, the construction of a diagram similar to Figure 9 for the particular protective barrier would provide an indication of the size of the damaged region in the barrier. Clearly, this requires knowledge of the strain wave propagation mechanics for the actual barrier configuration used, with the square-packed array of steel cylinders being only one possibility.

5. CONCLUSION

The experimental technique and results presented in this paper lay the foundation for an evolutionary understanding of the damage-inducing mechanisms for protective barriers that consist of an aggregate assembly of components. The barrier configuration that was examined for

13

6. REFERENCES

1. Baur, D. P., and M. D. Nagy. "Operation Manual for 50 mm Research Gun System." Technical Report UDR-TR-79-80, University of Dayton Research Institute, Dayton, OH, 1979.

2. Hohler, V., and A. J. Stilp. "Long Rod Penetration Mechanics." High Velocity Impact Dynamics, J. A. Zukas, ed., New York: John Wiley and Sons, Inc., pp. 377–378, 1990.

3. Tate, A. "A Simple Hydrodynamic Model for the Strain Field Produced in a Target by the Penetration of a High Speed Long Rod Projectile." Int. J. Engng. Sci., vol. 6, pp. 845–858, 1978.

INTENTIONALLY LEFT BLANK.

LIST OF SYMBOLS

V	Impact velocity (km/s)
a	Average strain empirical fitting parameter
b	Average strain empirical fitting parameter
d_c	Crater diameter (mm)
d_o	Pre-impact steel cylinder diameter (mm)
d_x	Steel cylinder diameter in x direction (mm)
d_y	Steel cylinder diameter in y direction (mm)
r	Radial distance (cylinder diameters)
x	Horizontal direction
y	Vertical direction
α	Crater diameter empirical exponent
ϵ	Steel cylinder strain
ϵ_{avg}	Average steel cylinder strain

INTENTIONALLY LEFT BLANK.

NO. OF
COPIES   ORGANIZATION

2   DEFENSE TECHNICAL INFO CTR
          ATTN DTIC DDA
          8725 JOHN J KINGMAN RD
          STE 0944
          FT BELVOIR VA 22060-6218

1   HQDA
          DAMO FDQ
          ATTN DENNIS SCHMIDT
          400 ARMY PENTAGON
          WASHINGTON DC 20310-0460

1   US MILITARY ACADEMY
          MATH SCI CTR OF EXCELLENCE
          DEPT OF MATHEMATICAL SCI
          ATTN MDN A MAJ DON ENGEN
          THAYER HALL
          WEST POINT NY 10996-1786

1   DIRECTOR
          US ARMY RESEARCH LAB
          ATTN AMSRL CS AL TP
          2800 POWDER MILL RD
          ADELPHI MD 20783-1145

1   DIRECTOR
          US ARMY RESEARCH LAB
          ATTN AMSRL CS AL TA
          2800 POWDER MILL RD
          ADELPHI MD 20783-1145

3   DIRECTOR
          US ARMY RESEARCH LAB
          ATTN AMSRL CI LL
          2800 POWDER MILL RD
          ADELPHI MD 20783-1145

          ABERDEEN PROVING GROUND

2   DIR USARL
          ATTN AMSRL CI LP (305)

19

1   COMMANDER
US ARMY MISSILE COMMAND
ATTN AMSMI RD ST WF
MIKE COLE
REDSTONE ARSENAL AL 35898-5247

1   US ARMY DUSA OPS RSCH
ATTN DANIEL WILLARD
102 ARMY PENTAGON
WASHINGTON DC 20310-0102

1   NAVAL RESEARCH LABORATORY
ATTN ANDREW WILLIAMS CODE 6684
4555 OVERLOOK AVE SW
WASHINGTON DC 20375

1   COMMANDER
NAVAL SURFACE WARFARE CENTER
DAHLGREN DIVISION
DAVE DICKINSON CODE G24
17320 DAHLGREN RD
DAHLGREN VA 22448-5000

1   DIRECTOR
LANL
ATTN LARRY SCHWALBE MS P915
PO BOX 1663
LOS ALAMOS NM 87545

1   SOUTHWEST RESEARCH INSTITUTE
ATTN C ANDERSON
PO DRAWER 28510
SAN ANTONIO TX 78284

1   ALLIANT TECHSYSTEMS INC
ATTN T HOLMQUIST MN11 2720
600 SECOND ST NE
HOPKINS MN 55343

1   ALME AND ASSOCIATES
ATTN MARVIN ALME
6219 BRIGHT PLUME
COLUMBIA MD 21044-3790

1   APPLIED RESEARCH ASSOCIATES INC
ATTN JEROME YATTEAU
5941 S MIDDLEFIELD RD SUITE 100
LITTLETON CO 80123

1   GRC INTERNATIONAL
ATTN TOM MENNA
PO BOX 6770
SANTA BARBARA CA 93160-6770

1   GRC INTERNATIONAL
ATTN WILLIAM ISBELL
5383 HOLLISTER AVE
SANTA BARBARA CA 93111

3   INST OF ADVANCED TECHNOLOGY
UNIVERSITY OF TX AUSTIN
ATTN MIKE NORMANDIA
STEVE BLESS
TOM KIEHNE
4030-2 W BRAKER LN
AUSTIN TX 78759

2   KAMAN SCIENCES CORP
ATTN J ELDER
J WILBECK
600 BLVD S SUITE 208
HUNTSVILLE AL 35802

1   KAMAN SCIENCES CORP
ATTN NASIT ARI
PO BOX 7463
COLORADO SPRINGS CO 80933-7463

ABERDEEN PROVING GROUND, MD

12   DIR, ARL
ATTN: AMSRL-WM-TC
       T BJERKE (5 CPS)
       R COATES
       W DE ROSSET
       K KIMSEY
       D SCHEFFLER
    AMSRL-WM-TD
       A DIETRICH, JR.
       K FRANK
       S SEGLETES

4   ERNST MACH INSTITUTE
         ATTN VOLKER HOHLER
         E SCHMOLINSKE
         E SCHNEIDER
         A J STILP
         ECKERSTRASSE 4
         D-7800 FREIBURG I BR 791 4
         GERMANY

1   FRENCH GERMAN RESEARCH INST
         ATTN H F LEHR
         POSTFACH 1260
         WEIL AM RHEIN D-79574
         GERMANY

1   FRENCH GERMAN RESEARCH INST
         ATTN P LEHMANN
         CEDEX 5 5 RUE DU GENERAL
         CASSAGNOU
         SAINT LOUIS 68301
         FRANCE

INTENTIONALLY LEFT BLANK.

REPORT DOCUMENTATION PAGE

Public reporting burden for this collection of information is estimated to average 1 hour per response, including the time for reviewing instructions, searching existing data sources, gathering and maintaining the data needed, and completing and reviewing the collection of information. Send comments regarding this burden estimate or any other aspect of this collection of information, including suggestions for reducing this burden, to Washington Headquarters Services, Directorate for Information Operations and Reports, 1215 Jefferson Davis Highway, Suite 1204, Arlington, VA 22202-4302, and to the Office of Management and Budget, Paperwork Reduction Project(0704-0188), Washington, DC 20503.

1. AGENCY USE ONLY (Leave blank)	2. REPORT DATE	3. REPORT TYPE AND DATES COVERED
	April 1997	Final, August 1994 - December 1995

4. TITLE AND SUBTITLE	5. FUNDING NUMBERS
Deformation of a Coarse-Aggregate Barrier Subjected to Ballistic Impact Loading	PR: 1L162618AH80

6. AUTHOR(S)

Todd W. Bjerke

7. PERFORMING ORGANIZATION NAME(S) AND ADDRESS(ES)	8. PERFORMING ORGANIZATION REPORT NUMBER
U.S. Army Research Laboratory ATTN: AMSRL-WM-TC Aberdeen Proving Ground, MD 21005-5066	ARL-TR-1346

9. SPONSORING/MONITORING AGENCY NAMES(S) AND ADDRESS(ES)	10. SPONSORING/MONITORING AGENCY REPORT NUMBER

11. SUPPLEMENTARY NOTES

12a. DISTRIBUTION/AVAILABILITY STATEMENT	12b. DISTRIBUTION CODE
Approved for public release; distribution is unlimited.	

13. ABSTRACT (Maximum 200 words)

An experiment-oriented investigation aimed at gaining insight and understanding of the physical phenomena that occur when a projectile impacts a thin barrier consisting of a uniform, coarse aggregate was performed at the U.S. Army Research Laboratory. The thin barrier target was an assembly of solid steel cylinders oriented in a 15-by-15 rod square-packed array. Each cylinder had a length-to-diameter ratio of 3.5 and a serial number imprinted on its rear surface to permit barrier reconstruction after each shot. The projectile consisted of a solid aluminum cylinder with a diameter of approximately 2.5 aggregate diameters and a length of 1.25 aggregate element lengths. The impact velocity was 2km/s. The data collected consisted of the crater size in the barrier (obtained from post-test reconstruction), plastic deformation of individual cylinders, and the residual penetrator length. A detailed analysis of the damage inflicted on the aggregate elements of the barrier was performed. Iso-strain contours were mapped on the face of the barrier to shed insight into the contact mechanics of the aggregate elements. A semi-empirical aggregate deformation model was created. The expected influence of impact velocity on aggregate deformation has been proposed and added to the semi-empirical model.

14. SUBJECT TERMS			15. NUMBER OF PAGES
impact, penetration, deformation			23
			16. PRICE CODE

17. SECURITY CLASSIFICATION OF REPORT	18. SECURITY CLASSIFICATION OF THIS PAGE	19. SECURITY CLASSIFICATION OF ABSTRACT	20. LIMITATION OF ABSTRACT
UNCLASSIFIED	UNCLASSIFIED	UNCLASSIFIED	UL

NSN 7540-01-280-5500

INTENTIONALLY LEFT BLANK.

USER EVALUATION SHEET/CHANGE OF ADDRESS

This Laboratory undertakes a continuing effort to improve the quality of the reports it publishes. Your comments/answers to the items/questions below will aid us in our efforts.

1. ARL Report Number/Author __ARL-TR-1346 (Bjerke)_____ Date of Report __April 1997_____

2. Date Report Received _____

3. Does this report satisfy a need? (Comment on purpose, related project, or other area of interest for which the report will be used.) _____

_____

_____

4. Specifically, how is the report being used? (Information source, design data, procedure, source of ideas, etc.) _____

_____

_____

5. Has the information in this report led to any quantitative savings as far as man-hours or dollars saved, operating costs avoided, or efficiencies achieved, etc? If so, please elaborate. _____

_____

_____

6. General Comments. What do you think should be changed to improve future reports? (Indicate changes to organization, technical content, format, etc.) _____

_____

_____

_____

CURRENT
ADDRESS

Organization _____

Name _____ E-mail Name _____

Street or P.O. Box No. _____

City, State, Zip Code _____

7. If indicating a Change of Address or Address Correction, please provide the Current or Correct address above and the Old or Incorrect address below.

OLD
ADDRESS

Organization _____

Name _____

Street or P.O. Box No. _____

City, State, Zip Code _____

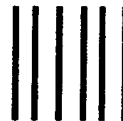(Remove this sheet, fold as indicated, tape closed, and mail.)
(DO NOT STAPLE)

DEPARTMENT OF THE ARMY

OFFICIAL BUSINESS

NO POSTAGE
NECESSARY
IF MAILED
IN THE
UNITED STATES

BUSINESS REPLY MAIL
FIRST CLASS PERMIT NO 0001,APG,MD

POSTAGE WILL BE PAID BY ADDRESSEE

DIRECTOR
US ARMY RESEARCH LABORATORY
ATTN AMSRL WM TC
ABERDEEN PROVING GROUND MD 21005-5066